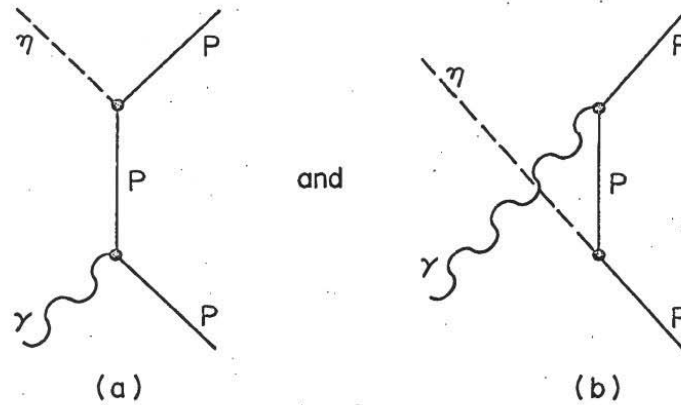




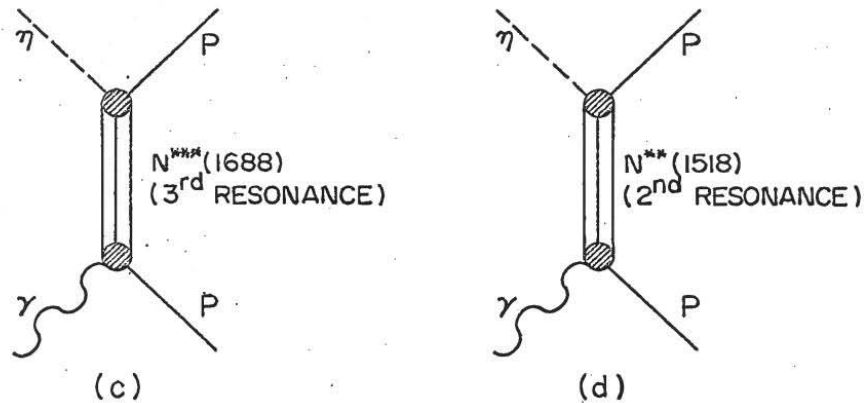
The CIT Era, Chez Heusch
#4 (Bruce Winstein)
May 6, 2002

Photoproduction at the Caltech Synchrotron

- Focus on Eta meson
- Resonances
 - Could they be photoproduced?
 - Coupling to eta vs pi?
- Regge Theory



NUCLEON BORN TERMS



ISOBAR TERMS

Figure 1.1 Diagrams of processes contributing to eta photoproduction

2 The DGLAP equation

The singlet DGLAP equation is^[7]

$$\frac{\partial}{\partial t} \mathbf{u}(x, Q^2) = \int_x^1 dz \mathbf{P}(z, \alpha_s(Q^2)) \mathbf{u}\left(\frac{x}{z}, Q^2\right) \quad (5)$$

where \mathbf{P} is the splitting matrix, $t = \log(Q^2/\Lambda^2)$ and

$$\mathbf{u} = \begin{pmatrix} x \sum_f (q_f + \bar{q}_f) \\ xg \end{pmatrix} \quad (6)$$

Write the Mellin transforms

$$\begin{aligned} \mathbf{u}(N, Q^2) &= \int_0^1 dx x^{N-1} \mathbf{u}(x, Q^2) \\ \mathbf{P}(N, \alpha_s(Q^2)) &= \int_0^1 dz z^N \mathbf{P}(z, \alpha_s(Q^2)) \end{aligned} \quad (7)$$

Then

$$\frac{\partial}{\partial t} \mathbf{u}(N, Q^2) = \mathbf{P}(N, \alpha_s(Q^2)) \mathbf{u}(N, Q^2) \quad (8)$$

A power contribution (1) to $F_2(x, Q^2)$ corresponds to a pole

$$\frac{\mathbf{f}(Q^2)}{N - \epsilon_0} \quad \mathbf{f}(Q^2) = \begin{pmatrix} f_q(Q^2) \\ f_g(Q^2) \end{pmatrix} \quad (9)$$

in $\mathbf{u}(N, Q^2)$. More generally, consider a contribution $x^{-\epsilon_0} f(x, Q^2)$. We assume that $f(x, Q^2)$ vanishes at $x = 1$ and is differentiable, for all Q^2 . Insert in the Mellin transform integral and integrate once by parts, to get

$$-\frac{1}{N - \epsilon_0} \int_0^1 dx x^{N-\epsilon_0} f_x(x, Q^2) \quad (10)$$

So there is a pole at $N = \epsilon_0$ with residue

$$-\int_0^1 dx f_x(x, Q^2) = f(0, Q^2) \quad (11)$$

With 4 active quark flavours and a flavour-blind hard pomeron, $f_q(Q^2) = \frac{18}{5} f_0(Q^2)$. We find^[6], on taking the residue of the pole at $N = \epsilon_0$ on each side of the Mellin transform (8) of the DGLAP equation,

$$\frac{\partial}{\partial t} \mathbf{f}(Q^2) = \mathbf{P}(N = \epsilon_0, \alpha_s(Q^2)) \mathbf{f}(Q^2) \quad (12)$$

We have previously^[4] fitted accurate ZEUS and H1 data in the range $x < 0.001$, $0.045 \leq Q^2 \leq 35$ GeV², together with data for $\sigma^{\gamma p}$. The result is

$$\epsilon_0 = 0.437 \quad (13)$$

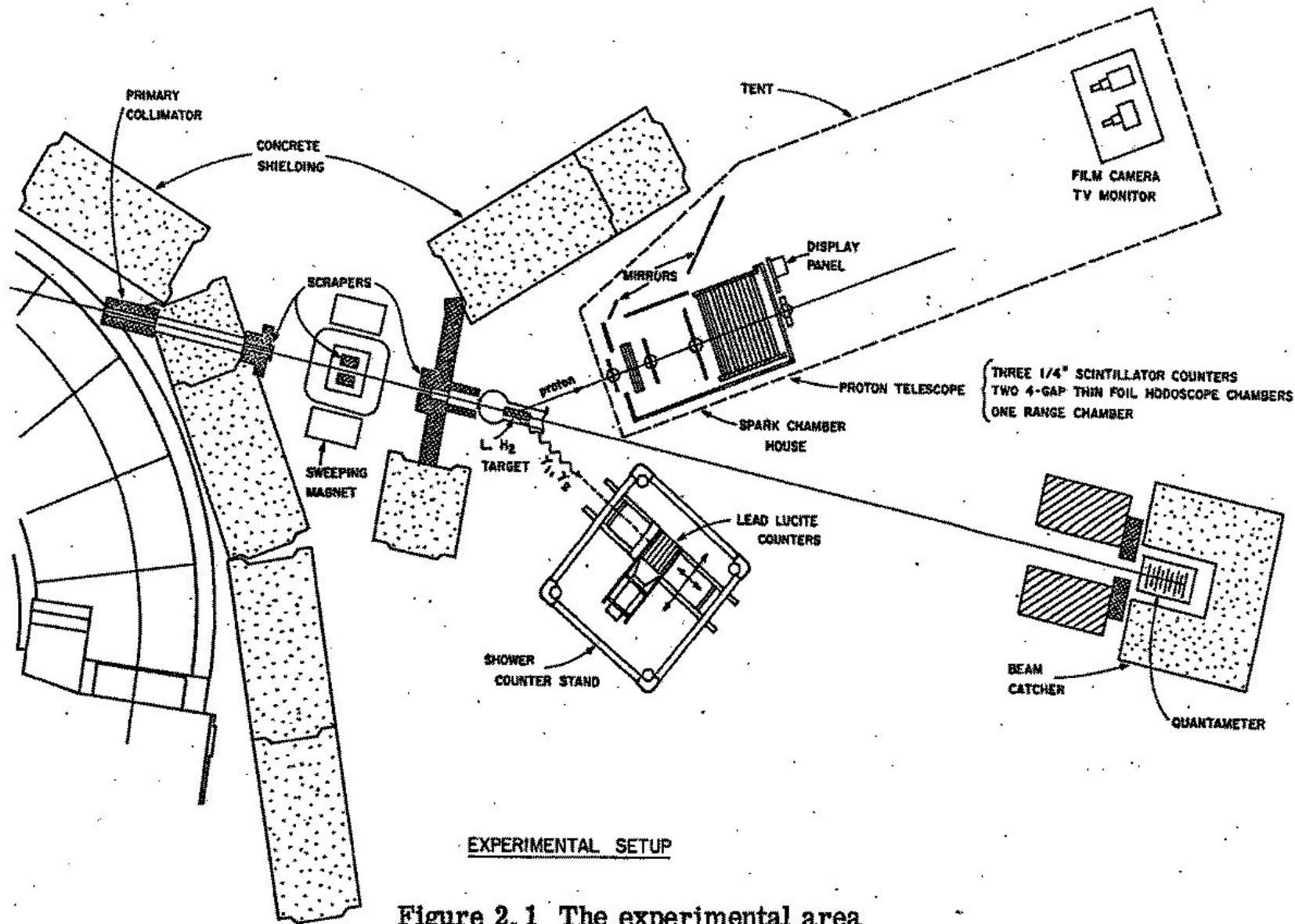


Figure 2.1 The experimental area

ETA MESON PHOTOPRODUCTION IN THE REGION
OF THE THIRD NUCLEON RESONANCE

Thesis by
Charles Y^{ung} Prescott

In Partial Fulfillment of the Requirements
For the Degree of
Doctor of Philosophy

California Institute of Technology
Pasadena, California
1966

On the other hand, there is no downward slope between 950 and 1100 MeV. Whether this is due to the presence of a shoulder caused by

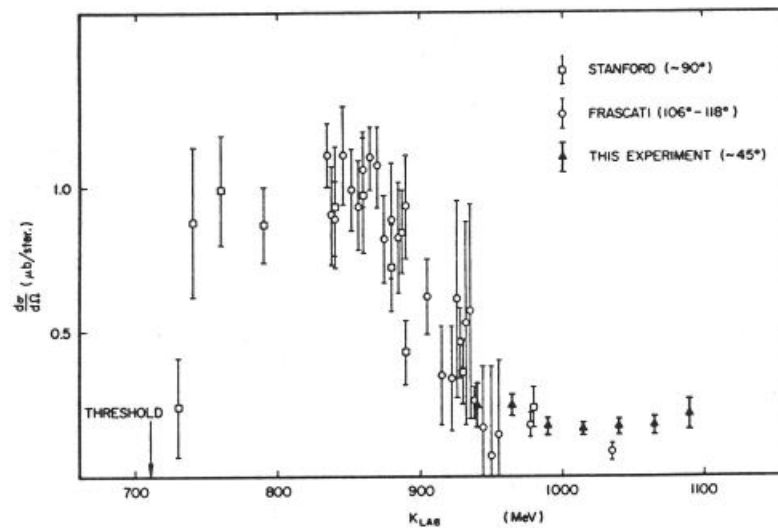


FIG. 3. Differential cross section for $\gamma + p \rightarrow p + \eta$. The Frascati⁶ and Stanford⁵ data were taken at angles around 90° c.m. This experiment was performed at 45° c.m. The energy dependence of the cross section resembles the $\pi^- + p \rightarrow n + \eta$ data.⁷⁻⁹ An enhancement in the 45° data, which would be expected from $N^{*++}(k = 1025 \text{ MeV})$ decay according to Fig. 1, is not seen.

ACKNOWLEDGMENTS

The success of this experimental effort must be directly attributed to cooperation in a group association. Clemens A. Heusch, as head of our group, conceived the experiment, laid down general guidelines for the experimental approach, supervised all details of construction of apparatus, and provided continuing motivation during the several years of experimental testing and construction. Elliott Bloom and Leon Rochester assisted in all aspects of the experiment, from equipment construction to data analysis, and deserve a full share of the credit. Walter Nilsson was an invaluable assistant, and every aspect of the apparatus shows his skillful craftsmanship, imaginative innovation, and patient attention to detail.

The author appreciates the continual support offered by R. L. Walker and A. V. Tollestrup. Both were sources of helpful suggestions and reliable advice. Many useful conversations with R. Dashen and D. Beder provided awareness of the connections of this experiment with points of interest in current theory. Assistance from the synchrotron crew under Larry Loucks, from Earle Emery, and from the synchrotron operators, headed by Al Neubieser, is gratefully acknowledged.

For financial support, the author is indebted to the National Science Foundation, the Atomic Energy Commission, and to the California Institute of Technology.

PHOTOPRODUCTION OF ETA MESONS FROM 950 TO 1100 MeV†

C. A. Heusch, C. Y. Prescott, E. D. Bloom, and L. S. Rochester

California Institute of Technology, Pasadena, California

(Received 18 July 1966)

This is a report on the first part of an experiment on photoproduction of η mesons at the Caltech 1.5-BeV electron synchrotron.¹ The η meson, whose mass and quantum numbers were established in bubble-chamber work in πN and KN interactions ($M_\eta = 548 \pm 1$ MeV, $J^{PC} = 0^{-+}$, $C = +1$), was later observed in photoproduction by Bacci *et al.* at Frascati.² The purposes of our experiment were to extend cross-section data to higher energies and, specifically, to investigate a possible contribution of the isobar diagram, Fig. 1, to the photoproduction mechanism. Since the space-time properties of the η meson are the same as those of the π^0 [both particles occupy the weight-2 position in the pseudoscalar-meson octet of SU(3)], the cross-section contributions due to this diagram should, except for kinematical differences, closely resemble each other. Using unbroken SU(3) the invariant coupling ratio can be predicted and a comparison carried out if the contribution of the diagram can be isolated.³

The $N^{*++}(1688$ MeV) has quantum numbers $T = \frac{1}{2}$, $J^P = \frac{5}{2}^+$. The angular-distribution data from π^0 photoproduction⁴ show the dominance of an $F_{5/2}$ wave, with maxima at 40° and 140° c.m. angles. Consequently, we chose c.m. angles around 45° for our investigation of η photoproduction. Measurement at 90° c.m. would make isolation of the contribution from the diagram in Fig. 1 hopeless.

The observation of η production by photons having a bremsstrahlung spectrum is handicapped by the presence of large competing background processes. We, therefore, chose a detection method with the intention of optimizing determination of the kinematical parameters of the final state. All final-state particles of the process

$$\gamma + p \rightarrow p + \eta^0 (\eta^0 \rightarrow 2\gamma)$$

were detected [branching ratio $\Gamma(\eta \rightarrow 2\gamma)/\Gamma(\eta \rightarrow \text{all decays}) = 38.6\%$ ⁵]. The general layout of the experiment is as follows: the bremsstrahlung beam from the synchrotron, collimated and passed through a sweeping magnet, interacts in a liquid hydrogen-target (containing

approximately 1 g/cm^2 liquid hydrogen) before being monitored by a Wilson-type quantameter. The recoil protons emerging from the target pass through a sequence of scintillation counters and thin-foil spark chambers, and are required to stop in a range-determining thick-plate spark chamber. This system fully determines the four-momentum of the recoil proton.⁶

The η is identified by detecting both decay photons from its $\gamma\gamma$ decay mode, observed in a plane perpendicular to the production plane. Each decay photon was detected in shower counters consisting of lead-lucite Čerenkov sandwiches.⁷ The shower counters were placed at the lab angles for the symmetrical decay of the η ($\sin^2 \theta_{\text{sym}} = m_\eta/E_\eta$). Each shower-counting system is preceded by (a) two veto counters in fast coincidence, to insure that a neutral particle initiated the observed pulse in the shower counter, (b) two radiation lengths of lead which convert most of the photons, and (c) a bank of scintillators which detect the converted photon and define the lab production angle. Information obtained from this apparatus, together with the four-momentum of the proton, overdetermines the entire final state sufficiently to make a suppression of backgrounds effective. A fast three-fold master coincidence ($\gamma_1 \gamma_2 p$) triggered the spark chambers; all data obtained were digitally displayed in the photographic frame and constantly monitored with a closed-circuit TV system. Pulse-height calibrations were performed at regular intervals on all critical counters. The constancy of counting rates of individual counters and coincidence outputs provided a close check on the performance of the fast logic.

Experimental data were obtained for incoming γ energies between 950 and 1100 MeV at η production angles around 45° in the c.m. sys-

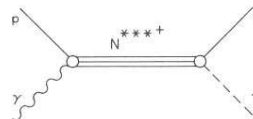


FIG. 1. Isobar diagram.

There is some evidence,⁶ however, which supports the use of a larger asymptotic normalization constant for the deuteron wave function than that of Eq. (2), and an increase of R by as much as a factor of 1.5 might result.

The numerical evaluation of $G(x)$ from Eq. (4) was done by Edward Monasterski using the IBM 7094 at the Goddard Laboratory for Theoretical Studies.

¹L. Meyer-Schützmeister, D. von Ehrenstein, and R. G. Allas, Phys. Rev. **147**, 743 (1966).

²Y. Hashimoto and W. P. Alford, Phys. Rev. **116**, 981 (1959). [These authors acknowledge a private communication from J. B. French.]

³R. J. Drachman, Phys. Rev. **132**, 374 (1963). [See also the erratum, Phys. Rev. **139**, AB4 (1965), which does not affect the present application.]

⁴The original form of the denominator should be

$$2\gamma \int_0^\infty dr e^{-2\gamma r} [1+F_0]^2 + 2\gamma \sum_{\text{even } L > 0} (2L+1)^{-1} \int_0^\infty dr e^{-2\gamma r} F_L^2.$$

Now, evaluating the first integral we have

$$2\gamma \int_0^\infty dr e^{-2\gamma r} [1+2F_0+F_0^2] = 1+4\gamma \int_0^\infty dr e^{-2\gamma r} F_0 + 2\gamma \int_0^\infty dr e^{-2\gamma r} F_0^2.$$

The second term vanishes because of the orthogonality of the ground-state function $|0\rangle$ and the first-order perturbation correction

$$F\varphi = \sum_{n \neq 0} \frac{|n\rangle \langle n|V|0\rangle}{E_0 - E_n}$$

⁵An estimate of the error incurred by neglecting $L > 1$ terms can be obtained by using the approximate form $F_L \alpha (r/2x)^L + 1/(L+1)$ for $r < 2x$, and $F_L = 0$ for $r > 2x$ (see Ref. 3, Sec. IV). Then it is easily shown, for example, that the $L=3$ term is about 5% of the $L=1$ contribution at $x=2$, and 3% at $x=4$.

⁶C. F. Clement, Phys. Rev. **128**, 2724 (1962).

SU(3) ASSIGNMENT AND COUPLING OF $N^*(1688)^* \dagger$

C. A. Heusch, C. Y. Prescott, and R. F. Dashen
California Institute of Technology, Pasadena, California

(Received 22 August 1966)

A comparison of the two reactions

$$\gamma + \rho - \eta + \rho$$

and

$$\gamma + \rho - \pi^0 + \rho$$

in the region of the third nucleon isobar $N^{***}(1688)$ has produced evidence that (1) $N^{***}(1688)$ is a member of a unitary octet, and (2) the D/F ratio, which relates the couplings $N^{***}N\pi$ and $N^{***}N\eta$, is similar to that which relates $NN\pi$ and $NN\eta$. One will note that (1) is in accord with the usual hypothesis that the N^{***} is the first Regge recurrence of the nucleon. Point (2) is not predicted by any existing theory but may have some simple dynamical origin or follow from some higher symmetry.

The above conclusions are arrived at as follows: An $I = \frac{1}{2}$ object decaying into πN (like N^{***}) must, in SU(3), belong to $\underline{8}$, $\underline{10}^*$, or $\underline{27}$. Of these possible assignments, we may immediately rule out $\underline{10}^*$ since $\gamma + \rho - \underline{10}^*$ is forbidden by SU(3)¹ whereas N^{***} is strongly observed in pion photoproduction. To decide between

$\underline{8}$ and $\underline{27}$, we compare the couplings $\gamma_{N^{***}N\pi^0}$ and $\gamma_{N^{***}N\eta}$; according to SU(3), the ratios are

$$\gamma_{N^{***}N\eta} / \gamma_{N^{***}N\pi} = 3 \text{ if } N^{***} \in \underline{27}, \\ = \frac{1}{3}(3-4\alpha)^2 \text{ if } N^{***} \in \underline{8}, \quad (1)$$

where $\alpha/(1-\alpha)$ is the D/F ratio. It is worth noting at this point that the ratio of the couplings can be small only if N^{***} belongs to an octet with $\alpha \sim \frac{2}{3}$.

To compare with experiment, we write²

$$R = \frac{\Gamma(N^{***} - \rho + \eta) f(q_\eta) \gamma_{\eta NN^{***}}}{\Gamma(N^{***} - \rho + \pi^0) f(q_\pi) \gamma_{\pi^0 NN^{***}}}, \quad (2)$$

where the f 's are kinematic factors. The ratio R can, of course, be determined by comparing the height of the N^{***} bump in the cross sections for $\gamma + \rho - \rho + \eta$ and $\gamma + \rho - \rho + \pi^0$. The kinematic factor, which is taken to be

$$f(q) = q \left(\frac{2}{q^2 + X^2} \right)^L, \quad (3)$$

ters 17, 59 (1965).

⁴M. Baldo-Ceolin, E. Calimani, S. Ciampolillo, G. Filippi-Filosofo, H. Huzita, F. Mattioli, and G. Miari, *Nuovo Cimento* 38, 684 (1965).

⁵P. Franzini, L. Kirsch, P. Schimdt, J. Steinberger, and R. J. Plano, *Phys. Rev.* 140, B127 (1965).

⁶L. Feldman, S. Frankel, V. L. Highland, T. Sloan, O. B. Van Dyck, W. D. Wales, R. Winston, and D. M. Wolfe, *Phys. Rev.* 155, 1611 (1967).

⁷B. M. K. Nefkens, A. Abashian, R. J. Abrams, D. W. Carpenter, G. P. Fischer, and J. H. Smith, *Phys. Letters* 19, 706 (1966).

⁸Our correction uses the theoretical estimate for the $\pi^+ \pi^- \gamma$ rate calculated by M. Bég, R. Friedberg, and J. Schultz as quoted in Ref. 5. Events which fit $\pi^+ \pi^- \gamma$ with a γ momentum, in the K^0 rest frame, of less than 50 MeV/c have been removed from the sample. This cut results in a 2% loss of leptonic decays.

⁹N. P. Samios, *Phys. Rev.* 121, 275 (1961).

¹⁰We use $\delta = -0.58h/c^2 \tau_S$, $\lambda_S = 1.18 \times 10^{10} \text{ sec}^{-1}$, and $\lambda_T = 1.85 \times 10^7 \text{ sec}^{-1}$.

¹¹Experiments are in progress to measure the charge

asymmetry in $K_L \rightarrow \pi e \nu$ (J. Steinberger et al. at Brookhaven National Laboratory) and in $K_L \rightarrow \pi \mu \nu$ (M. Schwartz et al. at Stanford Linear Accelerator Center) in order to resolve the ambiguity in the Wu-Yang description of the neutral K system. One solution predicts an asymmetry which would be observed in these experiments, while the other does not, but the effects could, in principle, be suppressed by $\Delta S = -\Delta Q$ amplitudes. Our experiment rules out a suppression from these amplitudes of more than 10 to 20%.

¹²If we ignore the charge of the lepton in the likelihood fit, we still obtain a two-standard-deviation violation. A χ^2 test to the total lepton time distribution yields for no violation $P(\chi^2) = 1.5\%$ and for best estimates $P(\chi^2) = 34\%$. This also corresponds to a two standard effect.

¹³In a Monte Carlo study of experiments, in which 86 positive leptons and 57 negative leptons were generated with $x = \phi = 0$, only 6% of the experiments resulted in a violation more significant statistically than our experiment.

¹⁴G. H. Trilling, Argonne National Laboratory Report No. ANL 7130, 1965 (unpublished), p. 115.

RECOIL-PROTON POLARIZATION IN π^0 PHOTOPRODUCTION*

E. D. Bloom,† C. A. Heusch, C. Y. Prescott, and L. S. Rochester
California Institute of Technology, Pasadena, California

(Received 24 July 1967)

In this Letter, we wish to communicate the results of an investigation into the energy dependence of the polarization of the final-state proton in neutral pion photoproduction. The energy region covered extends from 750 to 1450 MeV/c incoming photon momentum, at π^0 c.m. angles around 60° .

The results of this experiment indicate a zero crossing of the 60° polarization in the energy region covered, and a very strong angular dependence. We have attempted to incorporate this information into a unified picture of π^0 photoproduction, making use of all the presently available experimental information.¹

In the absence of polarization data from π^0 photoproduction above ~ 900 MeV and outside the 90° region, we choose c.m. angles around 60° for the higher energies. This was done because, in a simple isobar model incorporating a possible elementary vector meson exchange,² it promised to yield the most significant information short of a fuller angular distribution (which was excluded by limitations on running and subsequent scanning time); and because our experimental method was best applicable in this region.

In order to obtain a pure sample of protons from π^0 photoproduction, we detected the recoiling proton and both decay photons of the π^0 . This procedure sufficiently overdetermines the kinematics so as to give us an event sample which is clean to better than 98%; also, it allows us to determine, within the resolution of our apparatus, the inelasticity of the analyzing scatter of the recoil proton.

The experimental procedure employed is the following: A bremsstrahlung beam from the 1.5-BeV California Institute of Technology electron synchrotron impinged on a liquid-hydrogen target. The recoil proton passed through three scintillation counters and two thin-foil spark chambers; it subsequently entered a modular spark chamber built out of modules of carbon plates of varying thickness and two-gap sparking units, which served as both a range and scattering chamber. The dimensions were chosen such that all protons are stopped in the chamber, whether they undergo a scatter off a carbon nucleus or not. Carbon was chosen as a scatterer, because its analyzing power has been extensively studied over the energy region of interest to us ($80 \text{ MeV} \leq T_p$

DIFFERENTIAL CROSS SECTIONS IN ETA PHOTOPRODUCTION FROM 0.8 TO 1.45 GeV*

E. D. Bloom,† C. A. Heusch, C. Y. Prescott, and L. S. Rochester
California Institute of Technology, Pasadena, California

(Received 8 July 1968)

The cross section for the process $\gamma p \rightarrow p\eta$ was studied from 0.8- to 1.45-GeV incident photon energy at center-of-mass angles from 50 to 90°. The data cover a range of energies well beyond previous measurements. The results will aid in the study of $I = \frac{1}{2}$ nucleon isobars.

In this experiment we measured the differential cross section of the process

$$\gamma p \rightarrow p\eta(\eta \rightarrow 2\gamma) \quad (1)$$

by detecting all three particles in the final state, at incoming photon energies from 0.8 to 1.45 GeV, and at η center-of-mass angles between 40 and 100°.

The photoproduction of eta mesons derives its interest from two features; first, it can proceed through the $I = \frac{1}{2}$ channel only, so that it provides an unambiguous probe for nucleon isobars of isospin $\frac{1}{2}$; second, the position of η meson as the isosinglet in the 0^- -meson SU(3) octet makes a comparison with the production of the $I = 1, I_3 = 0$ π^0 fruitful. Since the γp vertex conserves U spin, SU(3) symmetry predicts definite coupling ratios for various exchanges and intermediate states. These are features which cannot be directly extracted from π production, or from processes of the type $\pi p \rightarrow \pi N$ and $\pi p \rightarrow \eta n$.

Existing data on η production in γp and πp collisions show two distinctive details: a sharp rise above threshold and a rapid decrease of the cross section occurring after a plateau of ~150-MeV width.¹ The onset and slope of the decrease appear to be different in the πN - and γN -initiated reactions.² There is fair evidence that in the region of the cross-section maximum, the angular distribution of η production is consistent with isotropy.³ In addition, a flat cross-section region above the strong decrease spans the energy region of the nucleon isobar $N_{15}^{*++}(1688)$.⁴

Several authors have made an attempt to account for this structure of the production cross section in terms of the nucleon isobars known from πN scattering and π photoproduction.⁵ The steep rise above threshold and the apparent isotropy at the maximum of the cross section are ascribed to the formation and decay of the $N^*(S_{11}, 1570)$ which was observed, with high inelasticity, in πN scattering.⁶ However, the steep decrease of the cross section, as exhibited by the existing data, is hard to explain even with the addition of

other terms. There may be an admixture of a P_{11} state or of the $D_{13}(1512)$, although the latter is expected to be suppressed because of the angular momentum barrier. In addition, a specific search for the decay of the $F_{15}(1688)$ ⁴ yielded an upper limit which allowed the assignment of this isobar to an SU(3) octet with $J^P = \frac{5}{2}^+$.⁷ This SU(3) assignment, together with a ratio for symmetric to antisymmetric octet-octet coupling of $\alpha/(1-\alpha) \approx \frac{3}{2}$, accounts for the suppression of this intermediate state for the ηN final state.

In the present experiment we sought to (1) reduce the errors and fluctuations on the high-energy end of the ηN threshold enhancement, (2) obtain a limited angular distribution around the $F_{15}(1688)$ energy region in order to check for F - or D -wave effects, and (3) extend the cross-section measurements to as high an energy as the California Institute of Technology 1.5-GeV electron synchrotron would permit.

The detection system for the final-state proton consisted of a spark-chamber telescope for proton detection (two thin-foil chambers for track delineation, defining the production angles to ~0.3° and a modular range chamber to stop the protons and determine their kinetic energy with a typical resolution of about 4 MeV) and a sequence of scintillator counters with pulse-height discrimination for triggering. The etas were detected through their decay mode into two photons, if it occurred symmetrically in a plane roughly perpendicular to the production plane. The photons passed through veto counters, a lead converter two radiation lengths thick, crossed scintillator hodoscopes to record the shower locations, and a lead-Lucite Čerenkov shower counter.⁸ In this manner, the eta production and decay angles were determined to $\pm 0.5^\circ$, and a rough measurement of the individual shower energies was obtained for consistency purposes.

As indicated below, this procedure overdetermines the kinematics, and allows for an efficient suppression of the backgrounds which plague eta photoproduction measurements. All kinematical

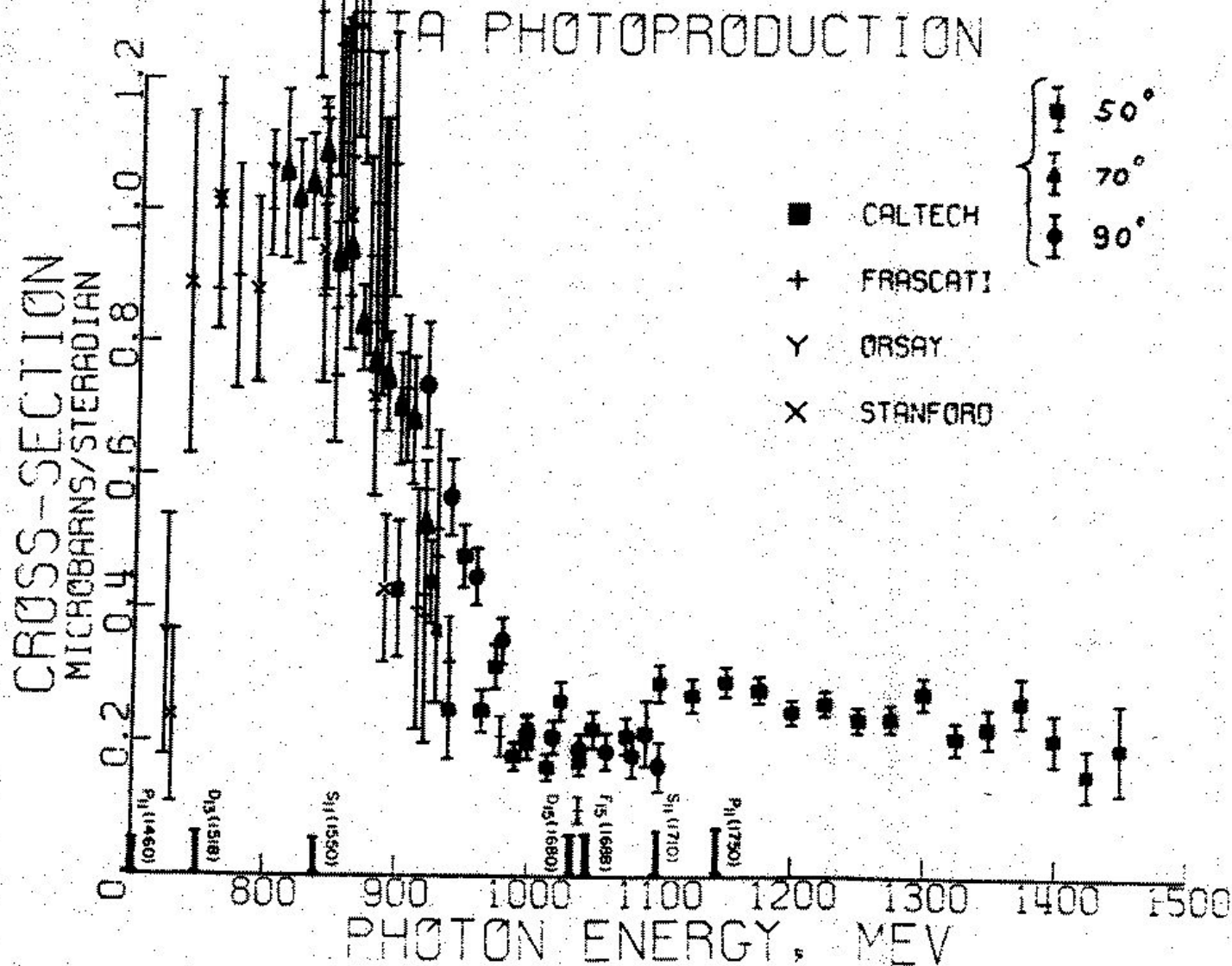


Figure 1.1 Eta photoproduction cross-section.

V. 3. ELECTRON AND PHOTON ENERGY MEASUREMENT UP TO 4 BeV

Clemens A. Heusch and Charles Y. Prescott
California Institute of Technology
Pasadena, California

We report here on work done on one aspect of the measurement of the energy of high-energy photons and electrons. We disregard such techniques as the deflection of electrons in magnetic fields and the various ionization methods, and concentrate on the fast measurement of electron and photon energies through their dissipation in electromagnetic cascade showers. Since buildup and decay of the showers are dominated by successive electron pair production and bremsstrahlung processes, the electron and photon cases are closely similar. We will mainly deal with the electron here, pointing out differences for the photon case where necessary.

In Figure 1 we see the parameters which describe a shower¹ initiated by a 1 BeV electron. The average number of electrons is plotted over the penetration depth. It starts with one in the electron case, zero in the photon case, and after the buildup region and maximum, decays exponentially. It is characterized by the position of the maximum ($\propto \log E_0/\epsilon_0$), with E_0 = incoming energy, ϵ_0 = critical energy of the shower-building material), the height of the maximum (roughly $\propto E_0$), the exponential decay constant (almost independent of E_0), and through the area under the curve ($\propto E_0$). The latter quantity,

$$\int_0^{\infty} \langle n(t) \rangle dt = T = \int_0^{\infty} n(t) dt,$$

where T is the total track length of shower particles, is approximately the same for the average shower and for any individual shower of the same E_0 , while the other characteristics show large fluctuations from the means. This relation is at the basis of all shower energy measurements. The working assumption is that the shower electrons dissipate equal amounts of energy along unit track length, irrespective of their energies. This should be true for any process used to detect the shower particles.

The two exploitable mechanisms for the revelation of T which we have looked into are the ionization loss of shower particles in scintillator plastics, and their Čerenkov radiation. The above assumption holds roughly for both processes as long as $\beta \approx 1$, for the Čerenkov process better than for the production of scintillation light.

Figure 2 shows the integrated pulseheight

spectra for π 's and electrons of $\beta \approx 1$, in scintillator plastic and in lucite, normalized at the median pulseheight.² The steeper front rise in the scintillator case demonstrates the large amount of light put out, compared with a relatively slow rise for both π 's and e's in the lucite. The π distributions, however, have long tails in the scintillator; so that for every case where identification of showering vs. non-showering particles is important, the selectivity of the lucite is preferable. If the scarcity of total light output and collection is the limiting factor, scintillation devices have to be considered. Shower detectors have to optimize the following parameters (Figure 3):

(a) number of sampling depths. Obviously, the more samplings we make along the penetration axis, the better will we beat shower statistics. The two limiting cases are 1) continuous sampling (as in high-Z, high-n, light-transmitting materials, e.g. lead glass and various fluids), and 2) one or two samplings by a scintillator behind some high-Z buildup material. The first method would be ideal, were it not that it presents severe light collection problems, has little adaptability to changing kinematical requirements, is expensive and hard to build. In the latter, distributions are broad due to shower fluctuations. We have, therefore, chosen a medium way, sampling sufficiently frequently to approximate 1) without running into its problems.

(b) Number of photons emitted per unit track length. In the Č case, this is a function of the optical index of refraction, n , which should be high. Scintillators put out ~40 times more light than lucite.

(c) Uniformity of light collection. This depends on the geometry of counter and light pipe, is excellent for lucite, poor for scintillator.

(d) Transmittance of light through radiator, favors UV transmitting lucite over other radiators.

(e) Shower containment, longitudinally and laterally, is purely a matter of geometry and can be adapted to incident energies.

Figure 4 shows a counter geometry we used for showers in the 100 MeV-5 BeV region. We built two identical counters which differed only in

Synchrotron Footage

3:00 - 4:01 PAN

4:01 - 5:39 ELECTRONICS

Clem Heusch's CIT Students

Eta Production	Prescott	1966
Pizero polarization	Bloom	May 4, 1967
Eta Production	Rochester	May 14, 1968
Eta Polarization	Winstein	May 21, 1970
Pizero production	Cheng	May 25, 1970
Pizero production (D)	Yellin	Feb 26, 1971
Eta production ($0^0, 180^0$)	McNeely	May 4, 1971
Gamma-He ₃ to pD	McDonald	May 24, 1972
pD to gamma He ₃	Kline	Oct 10, 1973

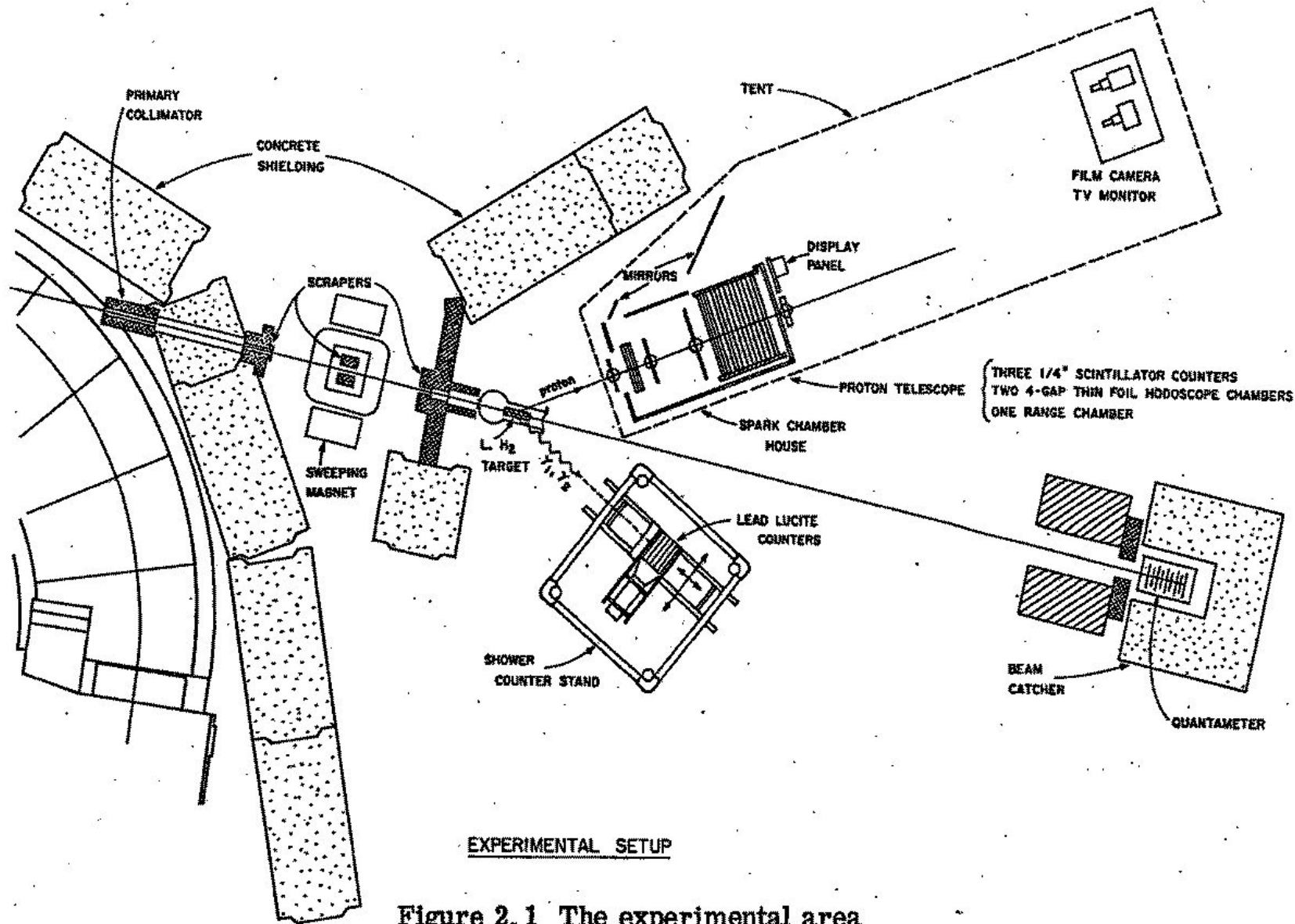


Figure 2.1 The experimental area

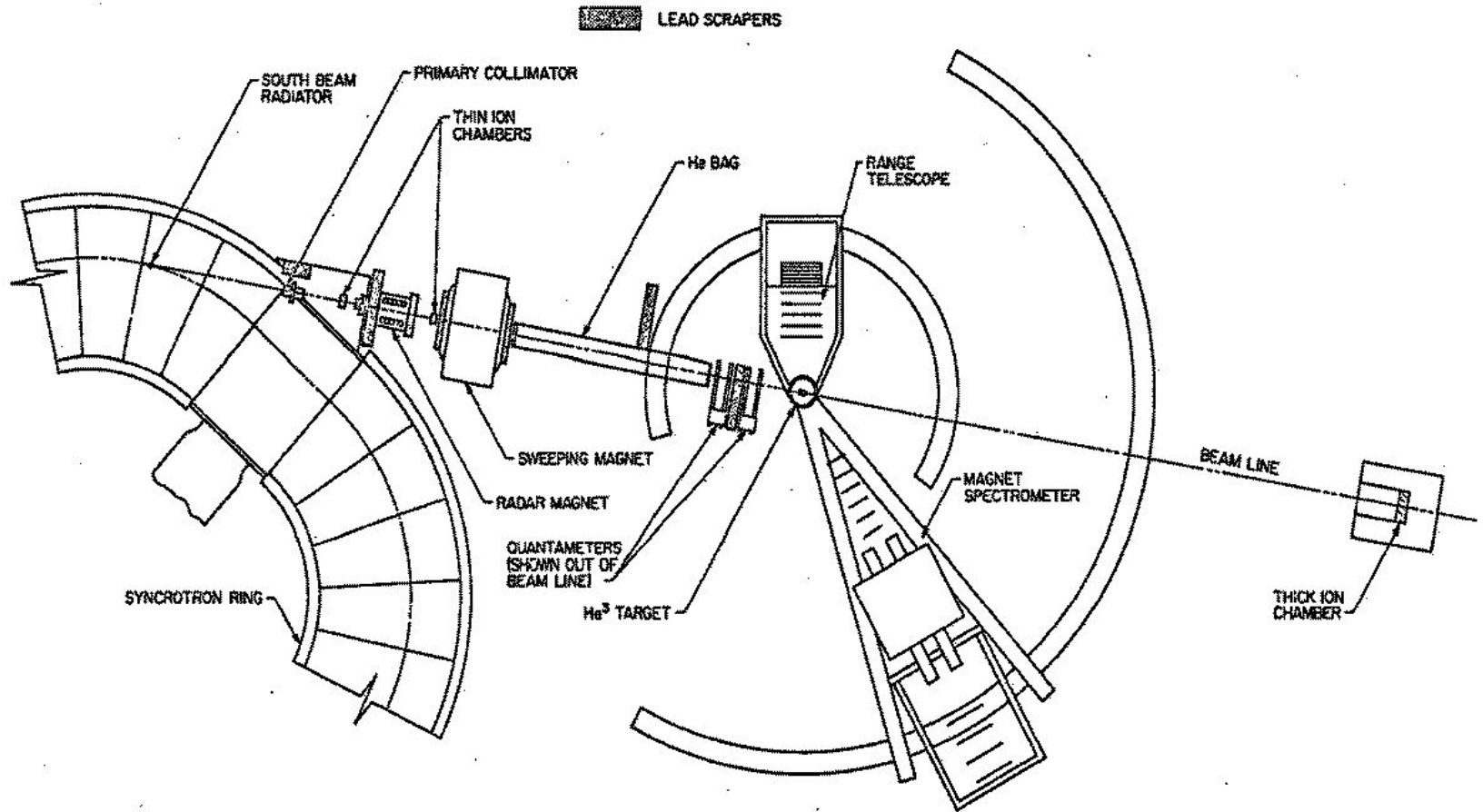


Figure 2.1 Layout of the Experiment

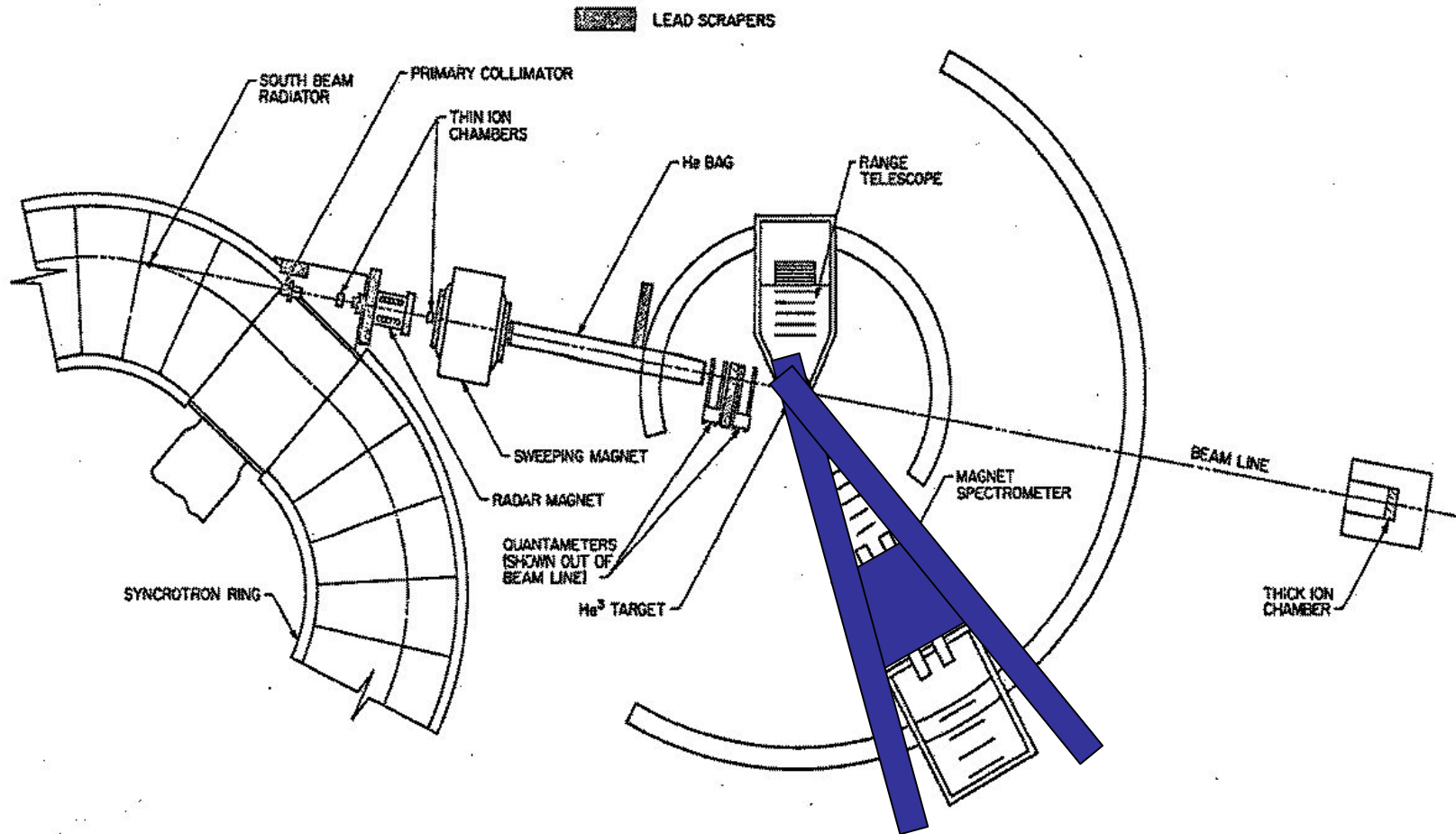


Figure 2.1 Layout of the Experiment

Multipole Analysis of Resonance Photoproduction*

JOHN BABCOCK

University of Minnesota, Minneapolis, Minnesota 55455

AND

JONATHAN L. ROSNER†

California Institute of Technology, Pasadena, California 91125

Received April 10, 1975

The single-quark-transition language of the Melosh transformation is used to extract reduced multipole matrix elements from three recent sets of photocouplings for non-strange baryon resonances. Magnetic dipole excitation of 56 , $L = 2$ resonances is found to be suppressed, a result to be expected if spin-orbit effects are weak. Suggestions are made for further reduction of uncertainties in the data.

INTRODUCTION

In the past 20 years, the reaction $\gamma N \rightarrow (\text{resonance}) \rightarrow \pi N$ has provided a tremendous amount of information about excited states of nucleons. Quite recently, the accumulation of a number of different types of data (involving polarized photons and/or targets) has enabled several groups [1-3] to extract photocouplings for most of the well-known nonstrange baryon resonances below 2 GeV. These photocouplings are of great interest at present. Thanks to the work of Melosh [4], we now have a clear-cut language in which to discuss the electromagnetic transitions of hadrons. This "single-quark-transition" theory seems to work surprisingly well [5-10], confirming the quark model assignments of the resonances to which it is applied and supporting conclusions regarding hadronic couplings obtained from other reactions such as elastic πN scattering and $\pi N \rightarrow \pi \Delta$ [11, 12].

The major excited multiplets to which one can apply the single-quark transition approach are denoted by their $(SU(6)_W, L)$ content: 70 , $L = 1$ and 56 , $L = 2$.

* Work supported in part by the Energy Research and Development Administration. Prepared under Contracts AT(11-1)-1764 and AT(11-1)-68 for the San Francisco Office.

† Permanent address: School of Physics and Astronomy, University of Minnesota, Minneapolis, Minnesota 55455.

An isobar model for η photo- and electroproduction on the nucleon

Wen-Tai Chiang^{a,*}, Shin Nan Yang^a, Lothar Tiator^b, Dieter Drechsel^b

^a Department of Physics, National Taiwan University, Taipei 10617, Taiwan

^b Institut für Kernphysik, Universität Mainz, 55099 Mainz, Germany

Received 15 October 2001; accepted 19 October 2001

Abstract

Eta photo- and electroproduction on the nucleon is studied using an isobar model. The model contains Born terms, and contributions from vector-meson exchanges and nucleon resonances. Our results are compared with recent eta-photoproduction data for differential and total cross sections, beam asymmetry, and target asymmetry, as well as electroproduction data. Besides the dominant $S_{11}(1535)$ resonance, we show that the second S_{11} resonance, $S_{11}(1650)$, is also necessary to be included in order to extract $S_{11}(1535)$ resonance parameters properly. In addition, the beam asymmetry data allow us to extract very small ($< 0.1\%$) $N^* \rightarrow \eta N$ decay branching ratios of the $D_{13}(1520)$ and $F_{15}(1680)$ resonances because of the overwhelming s -wave dominance. This model (ETA-MAID) is implemented as a part of the MAID program (the MAID program can be accessed from the webpage: <http://www.kph.uni-mainz.de/MAID/maid.html>). © 2002 Elsevier Science B.V. All rights reserved.

PACS: 13.60.Le; 14.20.Gk; 25.20.Lj; 25.30.Rw

Keywords: Eta meson; Photoproduction; Electroproduction; Isobar model; Nucleon resonances

1. Introduction

Eta photo- and electroproduction on the nucleon, $\gamma^* N \rightarrow \eta N$, provide an alternative tool to study N^* besides πN scattering and pion photoproduction. There are fewer resonances involved since the ηN state couples to nucleon resonances with isospin $I = 1/2$ only. Therefore, this process is cleaner and more selective to distinguish certain resonances than other processes, e.g., pion photoproduction. This provides opportunities to access less studied resonances and possibly the “missing resonances”.

* Corresponding author.

E-mail address: wtchiang@phys.ntu.edu.tw (W.-T. Chiang).

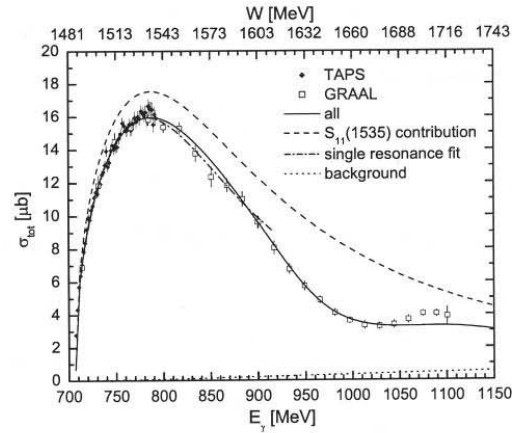


Fig. 4. Total cross section for $\gamma p \rightarrow \eta p$. The data are from TAPS [15] and GRAAL [29].

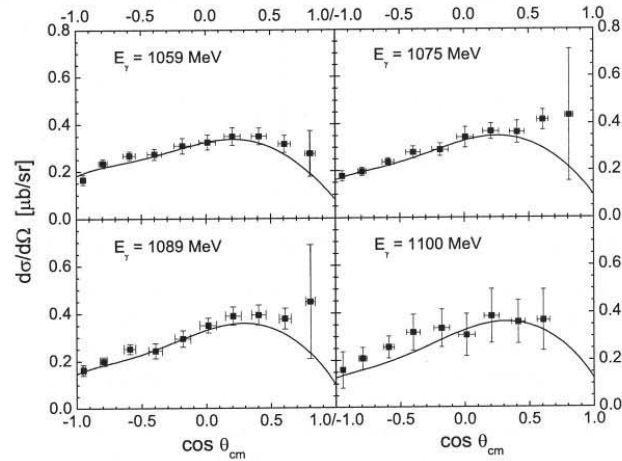


Fig. 5. Differential cross section for $\gamma p \rightarrow \eta p$ at energies between $E_{\gamma}^{\text{lab}} = 1050\text{--}1100$ MeV. The data are from GRAAL [29].

Fig. 4 shows that the background contribution is very small, and the total cross section is dominated by the $S_{11}(1535)$ at low energy. However, the contribution from the second resonance, $S_{11}(1650)$, can not be neglected. Even though a single S_{11} resonance can fit the low-energy data nicely up to $E_{\gamma}^{\text{lab}} = 910$ MeV (the dash-dotted curve in Fig. 4), it can by no means describe the higher-energy region. Moreover, the single resonance fit yields incorrect resonance parameters, as shown in Table 5. In fact, the decay width and photon

Acknowledgements, Thesis Students

- “provided me with continuing motivation and encouragement”
- “Insured that the project was a valuable and rewarding experience”
- “provided advice, active participation and constant encouragement”

Acknowledgements, Thesis Students, cont.

- “The presence of his creativity and experience was a necessary element in the success of our effort”
- “..his guidance, advice and high standards of excellence throughout the whole course of my stay at Caltech”
- “..owe greatest debt to Clem.. pervasive and salutary influence on all aspects, from conception to completion ”

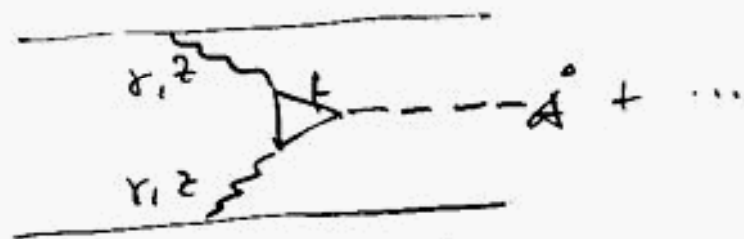
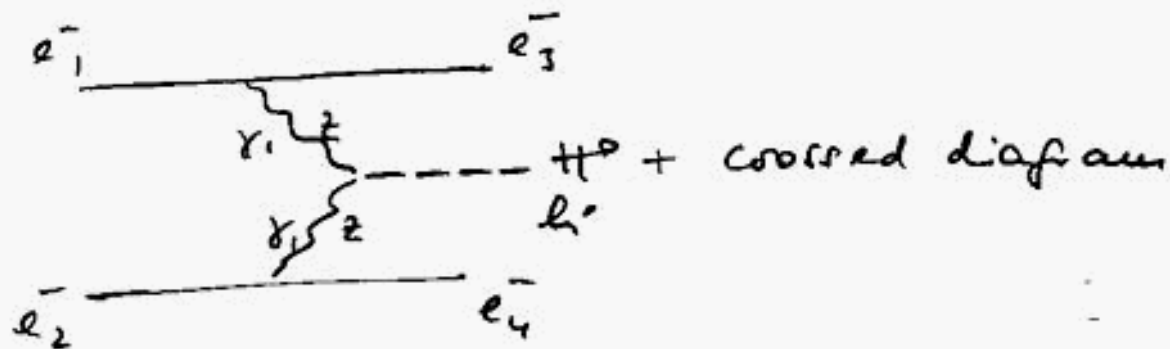
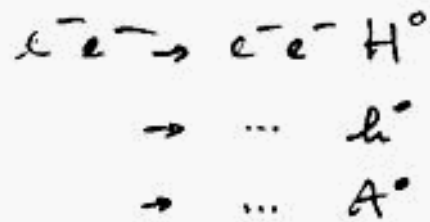
Acknowledgements, Thesis Students, cont.

- “.. Clemens Heusch, who rescued me from theoretical physics”

Data Analysis?

5:39 - 6:42 WAM IN COMPUTER
CENTER

WE LOOK AT CENTRAL PRODUCTION



WHICH HAS A NUMBER OF DISTINCTIVE

FEATURES:

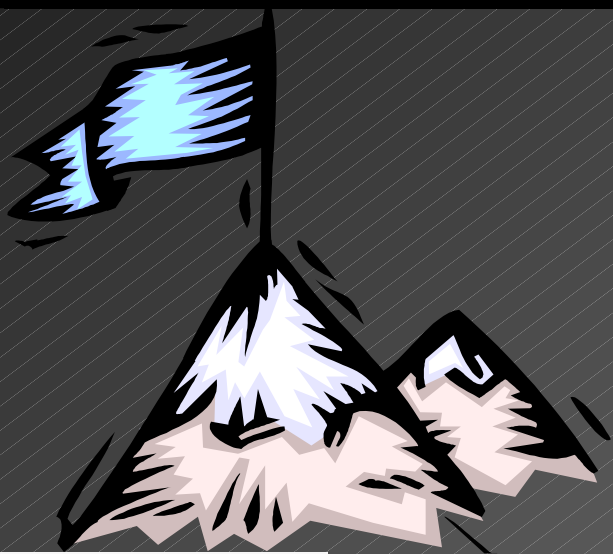
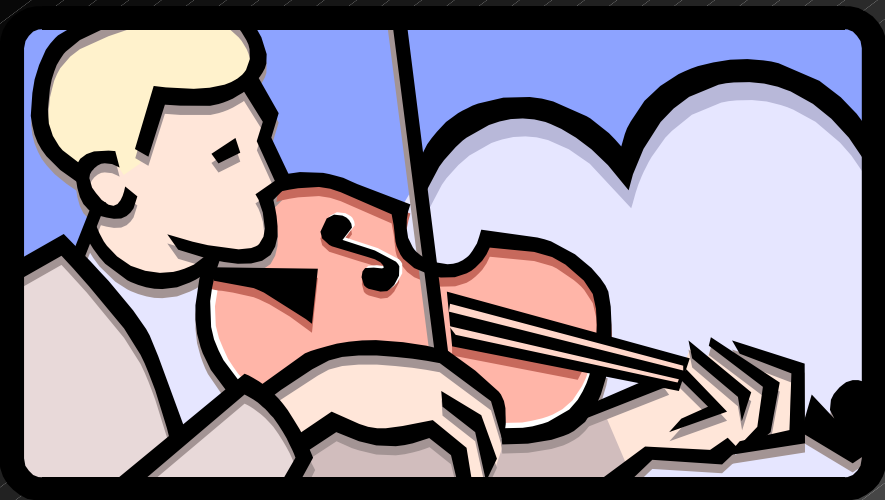
Thoughts on the Science

- We should have written a review article!
- Time between PhD Thesis and publication increased after 1970
- Went from BeV to GeV
- Results have stood the test of time!

Thoughts about Clem (and Karin)

- Shielded us from the politics
- Culture
- Generosity
- Loyalty
- Support





Best Wishes, Clem-, and Thanks
for Everything!